IJAME

Int. J. of Applied Mechanics and Engineering, 2023, vol.28, No.1, pp.11-22
DOI: 10.59441/ijame-2023-0002

MAGNETOHYDRODYNAMIC FLOW AROUND AN ELONGATED CYLINDER IN NON-DARCIAN POROUS REGIME WITH HIGHER ORDER CHEMICAL REACTION AND SORET/DUFOUR EFFECTS

UTPAL JYOTI DAS* and JUBI BEGUM
Department of Mathematics, Gauhati University, Assam, Guwahati-781014, INDIA
E-mail: jubi123begum@gmail.com

Here, we consider magnetohydrodynamic flow of an incompressible, time independent fluid past an elongated cylinder surrounded in a non-Darcian porous regime with magnetic flux supplied at an acute angle. The Soret/Dufour effects and the higher order chemical reactions are also included in the present study. The subsequent governing equations are resolved using the MATLAB-bvp4c method. The flow velocity appears to decrease with the growth of the Reynolds number, inertia parameter, magnetic field and angle of inclination of the magnetic flux, but improves with the Darcy number. The inertia parameter enhances the fluid temperature and skin friction. Further order of chemical reaction, Soret/ Dufour number plays a significant role in the system.

Key words: inertia parameter, magnetohydrodynamic, Soret number, Dufour number, porous medium, elongating cylinder, bvp4c.

1. Introduction

Fluids flowing in porous media (taking into account the non-Darcian effect) have wide applications in engineering processes and manufacturing technologies [1]. Pop and Rees [2] investigated the combined effect of a surface wave and the existence of inertia of fluid on a free convective flow brought by an upright hot surface in a fluid medium using a non-Darcy porous model. Cheng [3] studied the phenomena of natural convection and mass transfer near a vertically undulating surface both for Darcian and non-Darcian flow. Sheikhi *et al.* [4] studied the consequence of the non-Darcian parameter on water evaporation using a simulation method. Misra *et al.* [5] considered the non-Darcian model for a power-law fluid around a stretching sheet. Vedavathi *et al.* [6] studied the non-Darcian model and Nield's convective constraints.
Chemical reactions between foreign bodies and liquids occur in many important technological processes such as fuel combustion, iron production, glass and ceramic production, etc. Many industrial processes involve the transfer of flow and mass through the surface. Dispersed species can be produced or engrossed due to certain chemical species reacting with the surrounding fluid which can significantly affect the flow rate and therefore the characteristics and standard of the ultimate outcome. Cortell [7] examined the influence of chemical reaction on a time independent second- grade fluid flow past a semi-infinite impervious elongated sheet. Hayat *et al.* [8], Das [9] investigated the significance of chemical reaction for non-Newtonian liquids. M. Ramzan *et al.* [10] discussed the MHD fluid flow with the inclusion of a melting heat transfer with nonlinear chemical reaction across a slim needle in a porous system. Sarojamma *et al.* [11], Ly *et al.* [12], Shafique *et al.* [13] studied the impact of linear chemical reactions and authors like Sharma and Borgohain [14], Mythili and Sivaraj [15], Hosseinzadeh [16], Muthtamilselvan [17], Ramzan *et al.* [18] considered the impact of nonlinear chemical reaction on different flow problems.

The Soret effect occurs due to mass flux induced by heat differences while the Dufour effect occurs due to concentration gradient. The Soret effects associated with heat transfer and mass transfer with the consideration of radiation and magnetic field of a convective flow passing through a permeable stretched sheet

* To whom correspondence should be addressed

were analysed by El-Aziz [19]. Cheng [20] conducted a study on the Soret/Dufour effects in a free convection flow along a porous medium. EL-Kabeir [21] investigated the Soret/Dufour impacts on a stretched sheet using chemically reactive species. A numerical approach to chemically reacting laminar stream by considering Soret, Dufour effects and using convective borderline conditions was carried out by Makinde *et al.* [22]. Mathematical investigation of a magnetohydrodynamic fluid flow through upright permeable plates with the Soret and Dufour effect was carried out by Hasan and Hossain [23]. Recently, Das and Dorjee [24], Kumara *et al.* [25], Das [26], Balla *et al.* [27], and Kodi and Mopuri [28] contributed to this study.

In this study our aim is to investigate the influence of the non-Darcian and non-linear chemical reaction on an incompressible magnetohydrodynamic flow over an elongated cylinder surrounded in a porous regime. This paper is an extension of the work of Sharma and Borgohain [14] which incorporates the influences of an inclined magnetic field and non-Darcian porous medium.

2. Mathematical formulation

Consider a magnetohydrodynamic flow of a time independent, incompressible viscous fluid in an elongated cylinder surrounded by a non-Darcian porous regime. The magnetic flux is supplied at an acute angle β with a strength B_0 and a n-th order chemical reaction takes place in the presence of the heat source/sink parameter. The z^*-axis is taken along the cylinder axis and the r^*-axis is chosen in a radial direction and the cylinder radius is taken as b in the radial direction (Fig.1). Here, Forchheimer's extension is employed to designate the fluid flow in the permeable medium. The ambient temperature away from the cylinder surface is T_∞^* and the cylinder surface is kept at a constant temperature T_W^* with $T_W^* > T_\infty^*$.

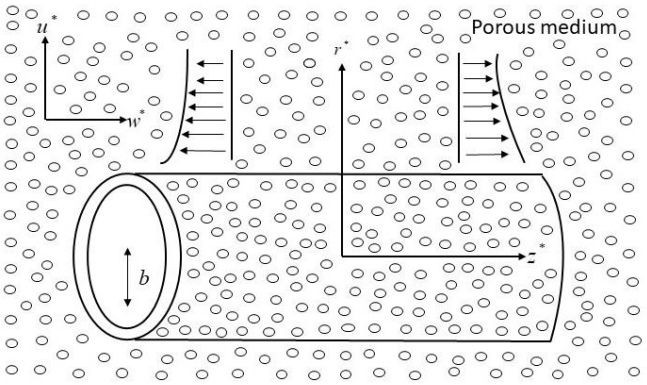

Fig.1. Physical diagram.

The governing equations, under the above assumptions (following [14]) become:

$$\frac{\partial w^*}{\partial z^*} + \frac{u^*}{r^*} + \frac{\partial u^*}{\partial r^*} = 0\,, \tag{2.1}$$

$$w^*\frac{\partial w^*}{\partial z^*} + u^*\frac{\partial w^*}{\partial r^*} = \nu\frac{\partial^2 w^*}{\partial r^{*2}} + \frac{\nu}{r^*}\frac{\partial w^*}{\partial r^*} - \frac{C_b}{\sqrt{k}}w^{*2} - \frac{\sigma {B_0}^2 w^*}{\rho}\sin^2\beta - \frac{\nu}{K}w^*\,, \tag{2.2}$$

$$w^*\frac{\partial u^*}{\partial z^*} + u^*\frac{\partial u^*}{\partial r^*} = -\frac{1}{\rho}\frac{\partial p^*}{\partial r^*} + \nu\frac{\partial^2 u^*}{\partial r^{*2}} + \frac{\nu}{r^*}\frac{\partial u^*}{\partial r^*} - \nu\frac{u^*}{r^{*2}} - \frac{\nu}{K}u^*\,, \tag{2.3}$$

$$w^*\frac{\partial T^*}{\partial z^*}+u^*\frac{\partial T^*}{\partial r^*}=\alpha\left(\frac{\partial^2 T^*}{\partial r^{*2}}+\frac{1}{r^*}\frac{\partial T^*}{\partial r^*}\right)+\frac{DK_T}{C_sC_P}\left(\frac{\partial^2 C^*}{\partial r^{*2}}+\frac{1}{r^*}\frac{\partial C^*}{\partial r^*}\right)+\frac{Q}{\rho c_p}\left(T^*-T_\infty^*\right), \tag{2.4}$$

$$w^*\frac{\partial C^*}{\partial z^*}+u^*\frac{\partial C^*}{\partial r^*}=D\frac{\partial^2 C^*}{\partial r^{*2}}+D\frac{1}{r^*}\frac{\partial C^*}{\partial r^*}+\frac{DK_T}{T_m}\left(\frac{\partial^2 T^*}{\partial r^{*2}}+\frac{1}{r^*}\frac{\partial T^*}{\partial r^*}\right)-k_1\left(C^*-C_\infty^*\right)^n. \tag{2.5}$$

Boundary conditions are:

$$\begin{aligned} &u^*=0,\quad w^*=W_W^*,\quad T^*=T_W^*,\quad \frac{dC^*}{dr^*}+\frac{K_T}{T_m}\frac{dT^*}{dr^*}=0 \quad \text{at} \quad r^*=b,\\ &w^*\to 0,\quad T^*\to T_\infty^*,\quad C^*\to C_\infty^* \quad \text{as} \quad r^*\to\infty. \end{aligned} \tag{2.6}$$

Here, $W_W^*=2cz^*$, c represents a positive constant.
Now, introducing (Sharma and Borgohain [14]) dimensionless variables as:

$$\begin{aligned} &\eta=\left(\frac{r^*}{b}\right)^2,\quad u^*=-cb\left(\frac{f(\eta)}{\sqrt{\eta}}\right),\quad w^*=2cz^*f'(\eta),\\ &\phi(\eta)=\frac{C^*-C_\infty^*}{C_\infty^*},\quad \theta(\eta)=\frac{T^*-T_\infty^*}{T_W^*-T_\infty^*}, \end{aligned} \tag{2.7}$$

using (2.7), equations (2.2), (2.4), (2.5) reduces to,

$$\eta f'''+f''+\mathrm{R}_e\left[ff''-f'^2\right]-\frac{1}{D_a}f'-\mathrm{R}_e Ff'^2-\frac{1}{4}H^2\sin^2\beta=0, \tag{2.8}$$

$$\eta\theta''+\theta'+D_F\,\mathrm{P}_r\left(\eta\phi''+\phi'\right)+\mathrm{R}_e\,\mathrm{P}_r\,f\theta'+S\,\mathrm{P}_r\,\theta=0, \tag{2.9}$$

$$\eta\phi''+\phi'+\mathrm{R}_e\,S_c\,f\phi'+S_rS_c\left(\theta'+\eta\theta''\right)-\gamma S_c\phi^n=0 \tag{2.10}$$

and (2.6) becomes:

$$\begin{aligned} &f=0,\quad f'=1,\quad \theta=1,\quad \phi'+S_rS_c\theta'=0 \quad \text{at} \quad \eta=1,\\ &f'\to 0,\quad \theta\to 0,\quad \phi\to 0 \quad \text{as} \quad n\to\infty \end{aligned} \tag{2.11}$$

where: $\mathrm{P}_r=\frac{\nu}{\alpha}$, the Prandtl number; $S_r=\frac{DK_T\left(T_W^*-T_\infty^*\right)}{\nu T_W^*T_\infty^*}$, the Soret number; $D_F=\frac{DK_T}{C_sC_p}\frac{C_\infty^*}{\nu\left(T_W^*-T_\infty^*\right)}$,

the Dufour number; $H = B_0 b\sqrt{\frac{\sigma}{\mu}}$, the magnetic parameter; $S = \frac{Qb^2}{4\nu\rho C_p}$, the heat source parameter; $S_c = \frac{\nu}{D}$, the Schmidt number; $\gamma = \frac{k_1 b^2 C_\infty^{*\,n-1}}{4\nu}$, the chemical reaction parameter; $D_a = \frac{4K}{b^2}$, the Darcy parameter; $F = \frac{C_b z^*}{\sqrt{k}}$, the inertia parameter, $\mathrm{R}_e = \frac{cb^2}{2\nu}$, the Reynolds number.

3. Results and discussion

Equations (2.8)-(2.10) with conditions (2.11) are solved by using MATLAB-bvp4c method. The following parameter values are used for the calculation:

$$\mathrm{R}_e = 1,\ D_F = 0.15,\ S_r = 0.4,\ \gamma = 0.02,\ \mathrm{P}_r = 7,\ n = 2,\ F = 0.2,$$

$$H = 2,\ \eta = 2,\ \beta = \frac{\pi}{3},\ S = 0.4,\ D_a = 1,\ S_c = 0.6.$$

Here it should be mentioned that the present problem reduces to the work of Sharma and Borgohain [14] when $F = 0,\ H = 0$ and $S = 0$. The results compared for $-\phi'(1)$ are presented in Tab.1 and are in good agreement.

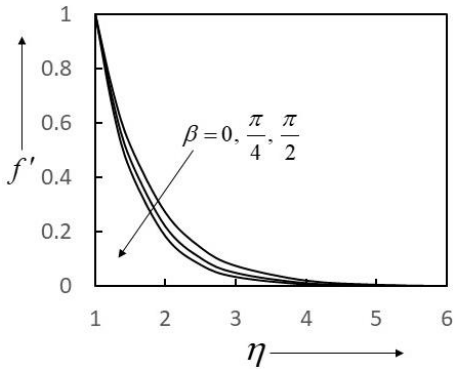

Fig.2. Effect of β on f'.

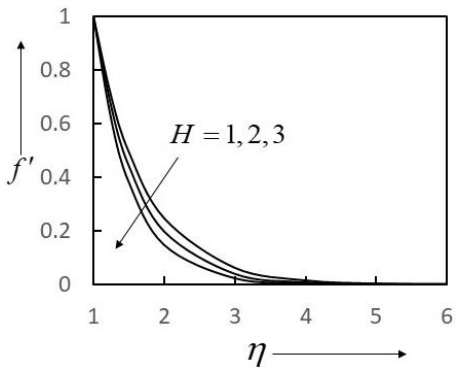

Fig.3. Effect of H on f'.

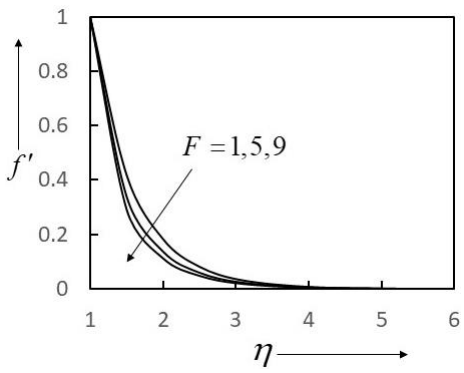

Fig.4. Effect of F on f'.

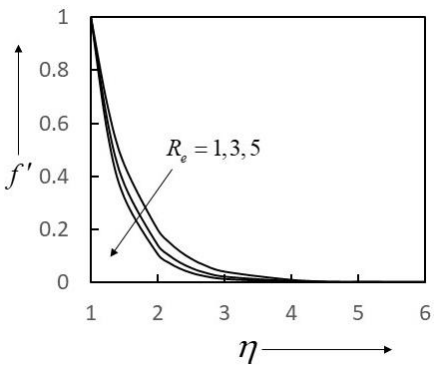

Fig.5. Effect of R_e on f'.

Figures 2-6 are plotted for fluid velocity against η to exhibit the influence of inclination of the magnetic flux (β), the Hartmann number (H), inertia parameter (F), Reynolds number (R_e) Darcy number (D_a), respectively. The figures show that the velocity declines exponentially from its highest on the cylindrical surface to its smallest estimate at the boundary layer edge. Figure 2 depicts that the velocity declines for the growing estimates of ϕ from $\beta = 0$ to $\beta = \frac{\pi}{2}$ through $\beta = \frac{\pi}{4}$ and thus $f'(\eta)$ decays. The sketch of the H effect in Fig.3 shows that H slows the velocity to an appreciable level, because of the resistive magnetic attraction exerted by the Lorentz force. The inertia parameter F which is resistive in nature reduces the flow velocity as shown in Fig.4. Figure 5 depicts that the augmentation in R_e reduces the flow velocity. This may be due to the increase in the Reynolds number; the viscous forces become less important and hence the flow velocity will get reduced.

Figure 6 shows that the higher the Darcy number D_a, the higher the flow velocity. As we increase the Darcy number, the capacity of the porous space increases, which subsequently increases the velocity profile.

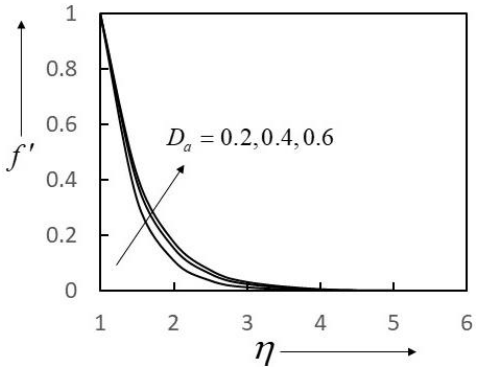

Fig.6. Effect of D_a on f'.

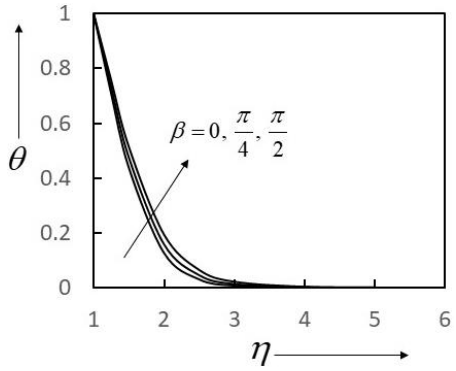

Fig.7. Effect of β on θ.

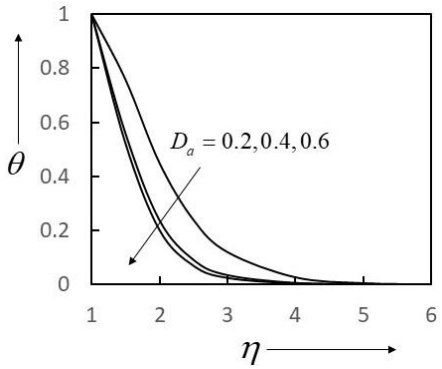

Fig.8. Effect of D_a on θ.

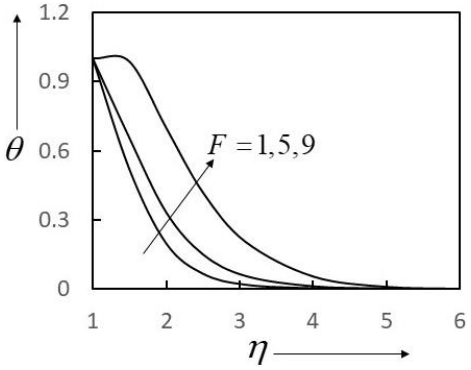

Fig.9. Effect of F on θ.

Figures 7-13 show the variation of temperature for the inclination of the magnetic flux (β), inertia parameter (F), Darcy number (D_a), heat source parameter (S), Schmidt number (S_c), Dufour number (D_F) and Prandtl number (P_r) respectively. The Figures show that the temperature drops exponentially from its peak on the surface of the cylinder to its lowest value at the boundary layer edge.

Figure 7 shows that an increasing value of β enhances the temperature inside the boundary layer. Figure 8 explains that the temperature decays with growing D_a values, although a different trend is prominent for increasing F values as illustrated in Fig.9.

Figure 10 shows that the temperature increases as the heat source (S) improves. Physically, the external heat source improves thermal conductivity, which leads to an amplification in temperature.

Figure 11 shows that an increase in S_c from $S_c = 0.75$ to $S_c = 1.78$ through $S_c = 1.16$ increases the temperature profile, while an increase in D_F (Fig.12) makes the temperature drop.

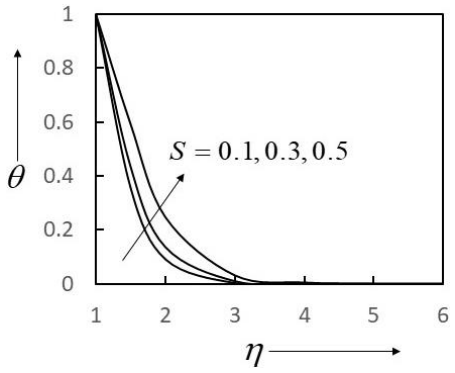

Fig.10. Effect of S on θ.

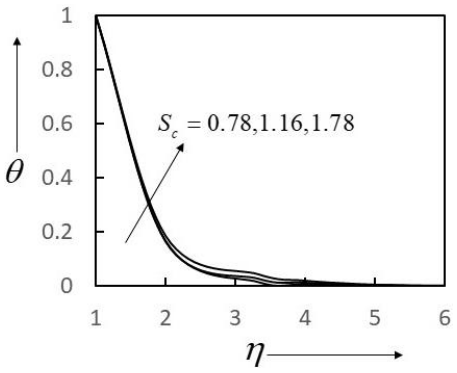

Fig.11. Effect of S_c on θ.

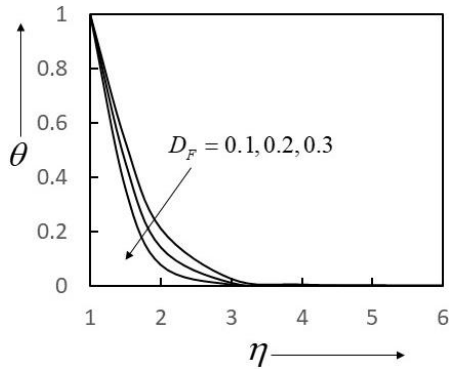

Fig.12. Effect of D_F on θ.

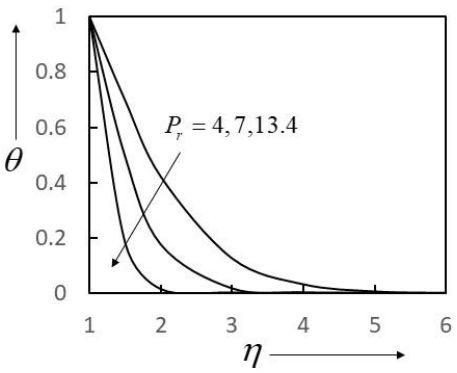

Fig.13. Effect of P_r on θ.

Figure 13 shows that the thickness of the boundary layer reduces for the rising values of P_r from $P_r = 4$ to $P_r = 13.4$ through $P_r = 7$. This reduction in temperature is due to the dominance of kinematic viscosity over thermal diffusivity.

Figures 14-17 illustrate the variation in concentration profiles against η under the influence of γ, S_c, S_r and D_F respectively. The concentration values are lower near the surface of the cylinder than those of the boundary layer edge, but increase sharply and reach a maximum around $\eta = 2$. Then they slowly decrease, reaching a constant value away from the surface. Figure14 shows that the chemical reaction parameter (γ) reduces the concentration profile. An enhancing effect of S_c on the concentration profile is seen in Fig.15. Physically, growth of S_c causes a decrease in molecular diffusivity which leads to an augmentation in concentration. The impact of the Soret number (Fig.16) and Dufour number (Fig. 17) causes a growth in the concentration profile.

The skin friction coefficient is proportional to $f''(1)$. Figures 18-19 represent the graph of $f''(1)$ against H for R_e and F. It is observed that the skin friction decreases significantly with the amplification of the magnetic parameter and R_e (Fig. 18) and F (Fig. 19).

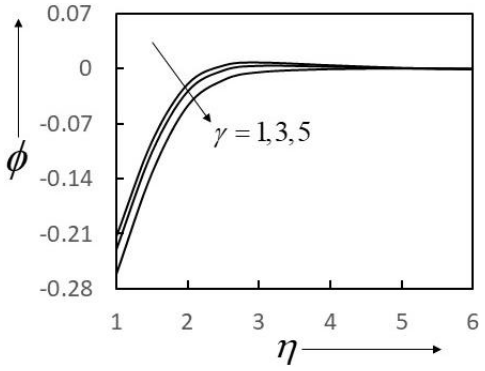

Fig.14. Effect of γ on ϕ.

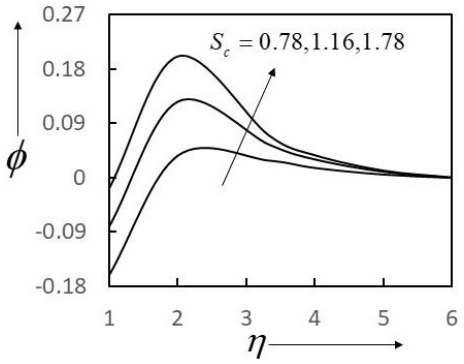

Fig.15. Effect of S_c on ϕ.

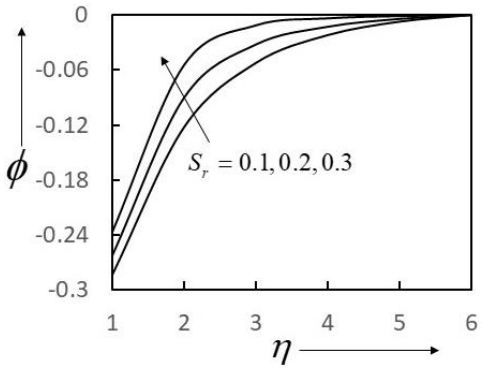

Fig.16. Effect of S_r on ϕ.

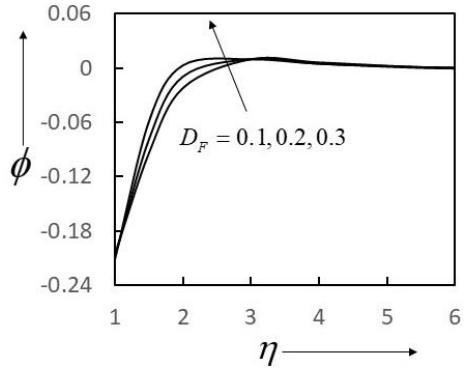

Fig.17. Effect of D_F on ϕ.

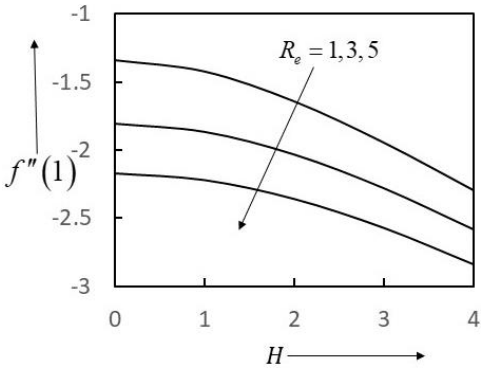

Fig.18. Skin friction vs. H.

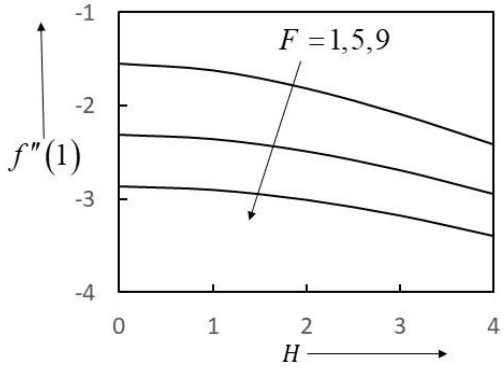

Fig.19. Skin friction vs. H.

The Nusselt number is proportional to $-\theta'(1)$. Figures 20 and 21 represent the graph of $-\theta'(1)$ against S for R_e and P_r respectively. We observe that the Nusselt number decreases significantly with increasing S but an opposite impact is observed for R_e and P_r.

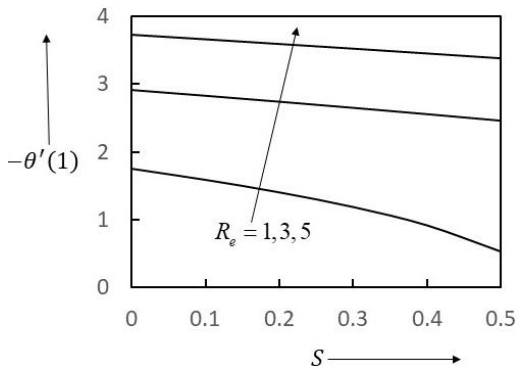

Fig.20. Local Nusselt number vs. S.

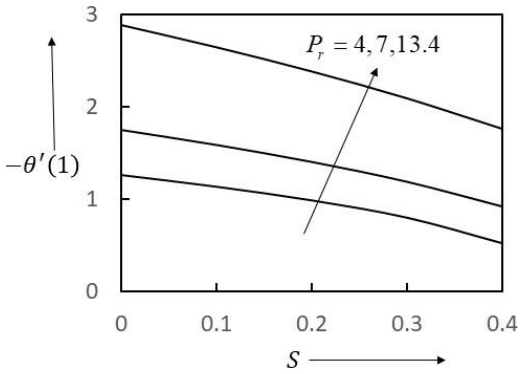

Fig.21. local Nusselt number vs. S.

Table 1. Comparison table for $-\phi'(1)$.

S_r	D_a	n	S_c	R_e	γ	P_r	D_F	$-\phi'(1)$ (Sharma and Borgohain [14])	$-\phi'(1)$ present result with $F=0, H=0, S=0$
0.01	*1*	*4*	*1.6*	*1*	*0.02*	*7*	*0.15*	*–0.0315*	*–0.0390*
0.01	*1*	*4*	*1.6*	*2*	*0.02*	*7*	*0.15*	*–0.0446*	*–0.0517*
0.01	*1*	*4*	*1.6*	*3*	*0.02*	*7*	*0.15*	*–0.0546*	*–0.0615*
0.01	*1*	*4*	*1.6*	*1*	*0.02*	*7*	*0.15*	*–0.0315*	*–0.0390*
0.01	*5*	*4*	*1.6*	*1*	*0.02*	*7*	*0.15*	*–0.0328*	*–0.0398*
0.01	*10*	*4*	*1.6*	*1*	*0.02*	*7*	*0.15*	*–0.0330*	*–0.0400*
0.04	*1*	*1*	*1.6*	*1*	*0.02*	*7*	*0.15*	*–0.1301*	*–0.1600*
0.04	*1*	*1*	*1.6*	*1*	*0.02*	*7*	*0.4*	*–0.1404*	*–0.1701*
0.04	*1*	*1*	*1.6*	*1*	*0.02*	*7*	*0.6*	*–0.1503*	*–0.1799*
0.01	*1*	*2*	*1.6*	*1*	*0.02*	*7*	*0.2*	*–0.0316*	*–0.0391*
0.4	*1*	*1*	*1.6*	*1*	*0.01*	*7*	*0.15*	*–2.3683*	*–2.6588*
0.4	*1*	*1*	*1.6*	*1*	*1*	*7*	*0.15*	*–2.4393*	*–2.6614*
0.4	*1*	*1*	*1.6*	*1*	*2.5*	*7*	*0.15*	*–2.5307*	*–2.6640*
0.01	*4*	*2*	*1.6*	*4*	*0.02*	*0.7*	*0.15*	*–0.0168*	*–0.0262*
0.01	*4*	*2*	*1.6*	*4*	*0.02*	*4*	*0.15*	*–0.0467*	*–0.0537*
0.01	*4*	*2*	*1.6*	*4*	*0.02*	*7*	*0.15*	*–0.0637*	*–0.0702*
0.01	*1*	*1*	*1.6*	*1*	*0.02*	*7*	*0.15*	*–0.0315*	*–0.0390*
0.01	*1*	*2*	*1.6*	*1*	*0.02*	*7*	*0.15*	*–0.0315*	*–0.0390*
0.01	*1*	*4*	*1.6*	*1*	*0.02*	*7*	*0.15*	*–0.0315*	*–0.0390*

The Sherwood number is proportional to $-\phi'(1)$. Figure 22 represents the graph of $-\phi'(1)$ against n for different values of the Soret numbers. We see that the Sherwood number decreases for $0 \le n < 1.2$ after which it remains almost stagnant. Also, the Sherwood number decreases due to the growth in the Soret number.

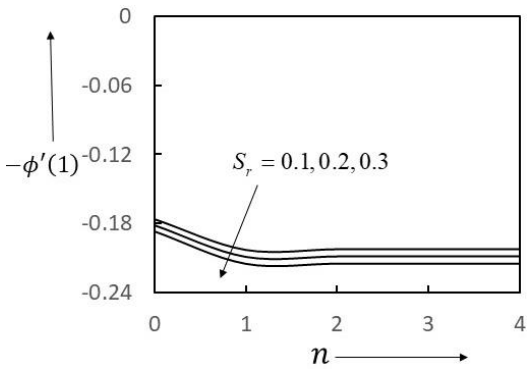

Fig.22. Sherwood number vs. n.

4. Conclusion

Main observations are:

1. The flow velocity declines with the growth of inertia, the magnetic field, angle of inclination of the magnetic flux, Reynolds number but rises with the Darcy number.
2. The temperature profile can be improved by increasing the inclination of the magnetic flux, inertia parameter, Schmidt number, and heat source, while the Dufour, Darcy and Prandtl numbers show the opposite trend.
3. The concentration profile can be amplified by escalating the Schmidt number, Soret number, Dufour number, whereas the chemical reaction parameters show the opposite trend.
4. A considerable decline in the skin friction is observed with the augmentation of the magnetic parameters and R_e.
5. The Nusselt number shows a significant decrease as S increases, but an opposite impact is observed for R_e and P_r.
6. The Sherwood number has a significant impact on the chemical reaction's order and on the Soret number.

Acknowledgements

The authors thank the management of the Department of Mathematics, Gauhati University and Department of Science and Humanities, Chirang Polytechnic for their continuous support to carry out this research work.

Nomenclature

$\mathrm{u}^*, \mathrm{w}^*$ – fluid velocity along the z^* and r^* -directions

K – permeability parameter

K_T – thermal diffusion ratio $\left(m^2 / s\right)$

D – mass diffusivity

T^* – temperature (K)

T_∞^* – ambient temperature (K)

T_W^* – constant temperature

T_m – mean fluid temperature

C^* – concentration $\left(mol / m^3\right)$

C_∞^* – ambient concentration $\left(mol / m^3\right)$

C_p – specific heat capacity $\left(J.kg^{-1}.K^{-1}\right)$

C_s – concentration susceptibility

K_1 – chemical reaction parameter

n – chemical reaction order

p^* – pressure (Pa)

R_e – Reynolds number

P_r – Prandtl number

S_c – Schmidt number

S_r – Soret number

D_a – Darcy number

D_F – Dufour number

H – Hartmann's number

S – heat source parameter

ν – kinematic viscosity $\left(m^2 / s\right)$

γ – non-dimensional chemical reaction parameter

α – thermal diffusivity $\left(m^2 / s\right)$

ρ – density $\left(kg / m^3\right)$

References

[1] Nield D.A and Bejan A.(2013): *Convection in Porous Media*.– Springer New York.

[2] Rees D.A.S. and Pop I. (1995): *Non-Darcy natural convection from a vertical wavy surface in a porous medium*.– Transport in Porous Media, vol.20, No.3, pp.223-234.

[3] Cheng C.Y.(2006): *Non-Darcy natural convection heat and mass transfer from a vertical wavy surface in saturated porous media*.– Applied Mathematics and Computation, vol.182, No.2, pp.1488-1500.

[4] Sheikhi E, Hashemi A and Kaffash A. (2015): *Effect of non-Darcy flow coefficient variation due to water vaporization on well productivity of gas condensate reservoir*.– Brazilian Journal of Chemical Engineering, vol.32, No.1, pp.237-245.

[5] Mishra S.R, Baag S., Dash G.C. and Acharya M.R. (2019): *Numerical approach to MHD flow of power-law fluid on a stretching sheet with non-uniform heat source*.– Nonlinear Engineering, vol.9, No.1, pp.81-93.

[6] Vedavathi N., Dharmaiah G., Kothuru V. and Gaffar S.A. (2021): *Numerical study of radiative non-Darcy nanofluid flow over a stretching sheet with a convective Nield conditions and energy activation*.– Nonlinear Engineering, vol.10, pp.159-176.

[7] Cortell R. (2007): *MHD flow and mass transfer of an electrically conducting fluid of second grade in a porous medium over a stretching sheet with chemically reactive species*.– Chemical Engineering and Processing: Process Intensification, vol.46, No.8 pp.721-728.

[8] Hayat T., Waqas M., Khan M.I. and Alsaedi A. (2017): *Impact of constructive and destructive chemical reaction in magnetohydrodynamics (MHD) flow of Jeffery liquid due to nonlinear radially stretched surface*.– Journal of Molecular Liquids, vol.225, pp.302-310.

[9] Das U.J. (2017): *Free convection heat and mass transfer flow for magnetohydrodynamic chemically reacting and radiating elastico-viscous fluid past a vertical permeable plate with gravity modulation*.– International Journal of Applied and Computational Mathematics, vol.3, No.3, pp.2021-2037.

[10] Ramzan M., Gul H., Kadry S., Lim C., Nam Y. and Howari F. (2019): *Impact of nonlinear chemical reaction and melting heat transfer on an MHD nanofluid flow over a thin needle in porous media*.– Applied Sciences, vol.9, No.24, pp.5492.

[11] Sarojamma G., Sreelakshmi K., Krishna Jyothi P. and Satya Narayana P.V. (2020): *Influence of homogeneous and heterogeneous chemical reactions and variable thermal conductivity on the MHD Maxwell fluid flow due to a surface of variable thickness*.– Defect and Diffusion Forum, vol.401, pp.148-163.

[12] Yu-Pei L., Shaheen N., Ramzan M., Mursaleen M., Sooppy Nisar K. and Malik M.Y. (2021): *Chemical reaction and thermal radiation impact on a nanofluid flow in a rotating channel with Hall current*.– Scientific Reports, vol.11, pp.19747.

[13] Shafique A., Un Nisa Z., Imran Asjad M., Nazar M. and Jarad F. (2022): *Effect of diffusion-thermo on MHD flow of a jeffrey fluid past an exponentially accelerated vertical plate with chemical reaction and heat generation*.– Mathematical Problems in Engineering, vol.2022, pp.6279498.

[14] Sharma B.R. and Borgohain D. (2014): *Influence of the order of chemical reaction and Soret effect on mass transfer of a binary fluid mixture in porous media*.– International Journal of Innovative Research in Science, Engineering and Technology, vol.3, No.7. pp.73-78.

[15] Mythili D. and Sivaraj R. (2016): *Influence of higher order chemical reaction and non-uniform heat source/sink on Casson fluid flow over a vertical cone and flat plate*.– Journal of Molecular Liquids, vol.216, pp.466-475.

[16] Hosseinzadeh Kh., Gholinia M., Jafari B. and Geravi A.G. (2018): *Nonlinear thermal radiation and chemical reaction effects on Maxwell fluid flow with convectively heated plate in a porous medium*.– Heat Transfer-Asian Research, vol.48, No.2, pp.744-759.

[17] Muthtamilselvan M., Ramya E. and Doh D. (2019): *Inclined Lorentz force effects on 3D micropolar fluid flow due to stretchable rotating disks with higher order chemical reaction*.– Journal of Mechanical Engineering Science, vol.233, No.1, pp.323-335.

[18] Ramzan M., Gul H., Kadry S., Lim C., Nam Y. and Howari F. (2019): *Impact of nonlinear chemical reaction and melting heat transfer on an MHD nanofluid flow over a thin needle in porous media*.– Applied Sciences, vol.9, No.24, pp.5492.

[19] Abd El-Aziz M. (2008): *Thermal-diffusion and diffusion-thermo effects on combined heat and mass transfer by hydromagnetic three-dimensional free convection over a permeable stretching surface with radiation*.– Physics Letters A, vol.372, No.3 pp.263-272.

[20] Cheng C.Y.(2009): *Soret and Dufour effects on natural convection heat and mass transfer from a vertical cone in a porous medium*.– International Communications in Heat and Mass Transfer, vol.36, No.10, pp.1020-1024.

[21] EL-Kabeir S. M. M. (2011):*Soret and Dufour effects on heat and mass transfer due to a stretching cylinder saturated porous medium with chemically-reactive species*.– Latin American Applied Research, vol.41, No.4, pp.331-337.

[22] Makinde O.D., Zimba K. and Anwar Beg O. (2012): *Numerical study of chemically-reacting hydromagnetic boundary layer flow with Soret/Dufour effects and a convective surface boundary condition*.– International Journal of Thermal & Environmental Engineering, vol.4, No.1, pp.89-98.

[23] Hasan M.M and Hossain T. (2019): *Soret and Dufour effects on the boundary layer magneto-fluid flow past an infinite vertical porous plate*.– Modelling Measurement and Control B, vol.88, pp.125-133.

[24] Das U.J. and Dorjee S. (2020): *Unsteady MHD oscillatory visco-elastic fluid flow through an inclined channel in presence of chemical reaction with Soret and Dufour effect*.– Indian Journal of Pure and Applied Physics., vol.58, No.9, pp.691-697.

[25] Kumara M.A., Reddy Y.D., Goud B.S. and Rao V.S. (2021): *Effects of Soret, Dufour, Hall current and rotation on MHD natural convective heat and mass transfer flow past an accelerated vertical plate through a porous medium*.– International Journal of Thermofluids, vol.9, pp.100061.

[26] Das U.J. (2021):*MHD Poiseuille flow with Soret and Dufour effects under slip boundary conditions*.– Latin American Applied Research, vol.51, No.3, pp.159-163.

[27] Balla C.S., Ramesh A., Kishan N. and Rashad A.M. (2021): *Impact of Soret and Dufour on bioconvective flow of nanofluid in porous square cavity*.– Heat Transfer, vol.50, No.1.

[28] Kodi R. and Mopuri O. (2022):*Unsteady MHD oscillatory Casson fluid flow past an inclined vertical porous plate in the presence of chemical reaction with heat absorption and Soret effects*.– Heat Transfer, vol.51, No.1, pp.733-752.

Received: September 15, 2022
Revised: January 29, 2023